

Organobismuth(III) Dihalides with T-Shaped Geometry Stabilized by Intramolecular N→Bi Interactions and Related Diorganobismuth(III) Halides

Albert P. Soran,[†] Cristian Silvestru,^{*,†} Hans J. Breunig,[‡] Gabor Balázs,[§] and Jennifer C. Green[§]

Facultatea de Chimie și Inginerie Chimică, Universitatea “Babeș-Bolyai”, 400028-Cluj-Napoca, Romania, Institut für Anorganische und Physikalische Chemie, Universität Bremen, 28334-Bremen, Germany, and Inorganic Chemistry Laboratory, University of Oxford, OX1 3QR Oxford, United Kingdom

Received December 20, 2006

Organobismuth(III) compounds containing (*N,C,N*)-pincer ligands were prepared and characterized both in solution and in the solid state. Compound RBiCl₂ **1** [R = 2,6-(Me₂NCH₂)₂C₆H₃] was obtained from RLi and BiCl₃ (1:1 molar ratio). RBiBr₂ **2** and RBiI₂ **3** were obtained by halogen-exchange reactions from **1**. Reaction of **1** with MeMgI afforded RBi(Me)I **4**. Compound R₂BiCl **5**, obtained from RLi and BiCl₃, is rearranged in solution to **1** and R₃Bi. The molecular structures of compounds **1–5** were established by single-crystal X-ray diffraction. All dihalides RBiX₂ show a T-shaped CBiX₂ core. They are the first stable compounds corresponding to the edge inversion “transition state” at the bismuth center, stabilized by two strong intramolecular N→Bi interactions in *trans* positions to each other, which contribute to an overall distorted square pyramidal (*N,C,N*)BiX₂ coordination geometry. The electronic structure of [2,6-(Me₂NCH₂)₂C₆H₃]BiCl₂ (**1**) was analyzed by density functional theory (DFT) calculations, which provide evidence that the stabilization of the square pyramidal geometry of bismuth is electronic rather than steric in nature.

Introduction

Interest in the chemistry of organobismuth(III) compounds has increased in recent years,¹ due to the potential biological activity and use, for example, as reagents and catalysts in organic synthesis (e.g., phenylation agent or mild oxidizing agents) and as precursors in advanced material science and heterometallic cluster chemistry (including compounds with bismuth–transition metal and bismuth–bismuth bonds). A recent review of the structural chemistry of organobismuth compounds² revealed that until 1998 relatively little attention was devoted to organobismuth compounds containing aryl groups *ortho*-substituted with CH₂NMe₂ or related pendent arms. Known examples of organobismuth(III) derivatives containing 2-(dimethylaminomethyl)-phenyl or related aryl groups with one pendent arm are RBi[C₆H₄{C(CF₃)₂O}-2],^{3,4} RR'BiCl (R' = 4-MeOC₆H₄, 4-MeC₆H₄, Ph, 4-ClC₆H₄, 1-naphthyl),⁵ RPhBiBr,⁵ [2-{Me₂N(Me)CH}C₆H₄]R'BiCl (R' = Ph, 1-naphthyl),^{5,6} R₃Bi,^{7a} R₂-BiCl,^{7b} RBiX₂ (X = Cl, I),^{7b} and [R₂Bi]⁺[PF₆]⁻^{7c} [R = 2-(Me₂NCH₂)C₆H₄]. A few examples of organobismuth(V) compounds, i.e., R(4-R'C₆H₄)₂Bi[C₆H₄{C(CF₃)₂O}-2] [R = 2-(Me₂NCH₂)-

C₆H₄; R' = Me, CF₃], were also described.⁸ By contrast, few organobismuth(III) compounds containing a 2,6-bis(dimethylaminomethyl)phenyl group, i.e., RBiCl₂ **1**⁹ and RBi[C₆H₄-{C(CF₃)₂O}-2] [R = 2,6-(Me₂NCH₂)₂-4-R'C₆H₂, R' = H, 'Bu],⁴ were reported until 1998. In all these compounds intramolecular N→Bi interactions were observed both in the solid state and in solution. Our recent work has been concerned with organobismuth compounds containing 2-(Me₂NCH₂)C₆H₄ and 2,6-(Me₂NCH₂)₂C₆H₃ groups,¹⁰ since these ligands are able to coordinate not only through the carbon atom but also through the pendent amino groups to the metal atom and thus provide well-protected hypervalent organobismuth compounds.¹¹ Indeed, we were able to isolate and to characterize low-valent organobismuth species such as *cyclo*-[2-(Me₂NCH₂)C₆H₄]₄Bi₄,^{10a} R₄Bi₂ [R = 2-(Me₂NCH₂)C₆H₄,^{10a} 2,6-(Me₂NCH₂)₂C₆H₃],^{10e} the first functionalized organobismuth(III) derivatives of the type [2-(Me₂NCH₂)C₆H₄]-

* To whom correspondence should be addressed. E-mail: cristi@chem.ubbcluj.ro.

[†] Universitatea “Babeș-Bolyai” Cluj Napoca.

[‡] Universität Bremen.

[§] University of Oxford.

(1) Suzuki, H.; Matano, Y., Eds. *Organobismuth Chemistry*; Elsevier Science B. V.: Amsterdam, 2001.

(2) Silvestru, C.; Breunig, H. J.; Althaus, H. *Chem. Rev.* **1999**, *99*, 3277.

(3) Yamamoto, Y.; Chen, X.; Akiba, K. *J. Am. Chem. Soc.* **1992**, *114*, 7906.

(4) Yamamoto, Y.; Chen, X.; Kojima, S.; Ohdoi, K.; Kitano, M.; Doi, Y.; Akiba, K. *J. Am. Chem. Soc.* **1995**, *117*, 3922.

(5) Suzuki, H.; Murafuji, T.; Matano, Y.; Azuma, N. *J. Chem. Soc., Perkin Trans. 1* **1993**, 2969.

(6) Murafuji, T.; Azuma, N.; Suzuki, H. *Organometallics* **1995**, *14*, 1542.

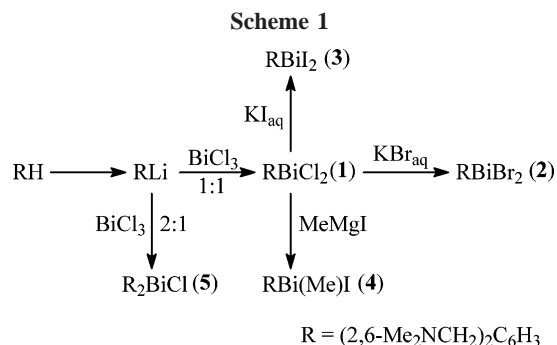
(7) (a) Kamepalli, S.; Carmalt, C. J.; Culp, R. D.; Cowley, A. H.; Jones, R. A.; Norman, N. C. *Inorg. Chem.* **1996**, *35*, 6179. (b) Carmalt, C. J.; Cowley, A. H.; Culp, R. D.; Jones, R. A.; Kamepalli, S.; Norman, N. C. *Inorg. Chem.* **1997**, *36*, 2770. (c) Carmalt, C. J.; Walsh, D.; Cowley, A. H.; Norman, N. C. *Organometallics* **1997**, *16*, 3597. (d) James, S. C.; Norman, N. C.; Orpen, A. G. *J. Chem. Soc., Dalton Trans.* **1999**, 2837.

(8) Yamamoto, Y.; Ohdoi, K.; Chen, X.; Kitano, M.; Akiba, K. *Organometallics* **1993**, *12*, 3297.

(9) Atwood, D. A.; Cowley, A. H.; Ruiz, J. *Inorg. Chim. Acta* **1992**, *198–200*, 271.

(10) (a) Balázs, L.; Breunig, H. J.; Lork, E.; Silvestru, C. *Eur. J. Inorg. Chem.* **2003**, 1361. (b) Balázs, L.; Stângă, O.; Breunig, H. J.; Silvestru, C. *Dalton Trans.* **2003**, 2237. (c) Breunig, H. J.; Gheşner, I.; Gheşner, M. E.; Lork, E. *Inorg. Chem.* **2003**, *42*, 1751. (d) Breunig, H. J.; Balázs, L.; Philipp, N.; Soran, A.; Silvestru, C. *Phosphorus, Sulfur Silicon* **2004**, *179*, 853. (e) Balázs, L.; Breunig, H. J.; Lork, E.; Soran, A.; Silvestru, C. *Inorg. Chem.* **2006**, *45*, 2341. (f) Fernández, E. J.; Laguna, A.; López-de-Luzuriaga, J. M.; Monge, M.; Nema, M.; Olmos, M. E.; Pérez, J.; Silvestru, C. *Chem. Commun.* **2006**, DOI: 10.1039/b613365g.

(11) Akiba, K., Ed. *Chemistry of Hypervalent Compounds*; Wiley-VCH: New York, 1999.



$\text{BiCl}[(\text{XPR}_2)(\text{YPR}'_2)\text{N}]$ ($\text{X}, \text{Y} = \text{O}, \text{S}, \text{Se}; \text{R}, \text{R}' = \text{Me}, \text{Ph}$),^{10b} and organobismuth heterocycles $(\text{RBiS})_2$ [$\text{R} = 2\text{-(Me}_2\text{NCH}_2\text{)-C}_6\text{H}_4, 2,6\text{-(Me}_2\text{NCH}_2)_2\text{C}_6\text{H}_3$].^{10d} We have also reported the unusual reaction of the dibismuthane $\text{R}_2\text{Bi-BiR}_2$ with oxygen leading to the formation of the first peroxo derivative [$2,6\text{-(Me}_2\text{NCH}_2)_2\text{C}_6\text{H}_3$]₂ $\text{Bi}_2(\text{O}_2)$ ^{10e} and [$2\text{-(Me}_2\text{NCH}_2)\text{C}_6\text{H}_4$]₂ $\text{BiAu-(C}_6\text{F}_5)_2$, a compound that exhibits the first metallophilic $\text{Au}^{\text{I}} \cdots \text{Bi}^{\text{III}}$ closed-shell interaction.^{10f}

In earlier reports, on the basis of multinuclear NMR solution studies of $\text{RBi}[\text{C}_6\text{H}_4\{\text{C}(\text{CF}_3)_2\text{O}\}_2]$ [$\text{R} = 2\text{-(Me}_2\text{NCH}_2)\text{C}_6\text{H}_4; 2,6\text{-(Me}_2\text{NCH}_2)_2\text{-4-R}'\text{C}_6\text{H}_2, \text{R}' = \text{H}, \text{tBu}$],^{3,4} Yamamoto et al. concluded that external (solvent molecules) or internal (intramolecularly coordinating groups) nucleophiles can considerably reduce the barrier for the edge inversion of bismuth(III) compounds through a “transition state” with a T-shaped (*C, O*)- CBi core. It should be noted here that the structure of the related organoantimony(III) derivative, $2,6\text{-(Me}_2\text{NCH}_2)_2\text{C}_6\text{H}_3\text{SbCl}_2$, indeed exhibits a T-shaped CSbCl_2 core, in this case the stabilization induced by the two internal coordinated nitrogen atoms from the pendent arms being so strong that an edge inversion “transition state” had become a ground state.^{7a}

Herein we report the synthesis, spectroscopic characterization, and crystal structures of the dihalides $2,6\text{-(Me}_2\text{NCH}_2)_2\text{C}_6\text{H}_3\text{-BiX}_2$ ($\text{X} = \text{Cl}, \text{Br}, \text{I}$), which are the first compounds with a T-shaped CBiX_2 core stabilized by two intramolecular $\text{N} \rightarrow \text{Bi}$ interactions. Some T-shaped organobismuth(III) halides with two intermolecular $\text{N} \rightarrow \text{Bi}$ interactions were already described.^{7d} Related compounds with a T-shaped CBiX_2 core stabilized by two intramolecular $\text{O} \rightarrow \text{Bi}$ interactions were recently described.¹² The stabilization of the overall square pyramidal geometry of bismuth is of electronic rather than steric origin, as indicated by the DFT calculations carried out on the dichloro derivative. The synthesis and structure of two related diorganobismuth(III) halides, $2,6\text{-(Me}_2\text{NCH}_2)_2\text{C}_6\text{H}_3\text{BiCl}$ and $2,6\text{-(Me}_2\text{NCH}_2)_2\text{C}_6\text{H}_3(\text{Me})\text{BiI}$, are also discussed.

Results and Discussion

Synthesis and Spectroscopic Characterization of $2,6\text{-(Me}_2\text{NCH}_2)_2\text{C}_6\text{H}_3\text{BiX}_2$ (1–3). The dichloride $2,6\text{-(Me}_2\text{NCH}_2)_2\text{C}_6\text{H}_3\text{BiCl}_2$ (**1**) was synthesized by a slightly modified and improved procedure of that previously reported by Cowley and co-workers (for details, see Supporting Information).⁹ In order to investigate the influence of the nature of the halogen on the coordination sphere of the bismuth center, several experiments were carried out (Scheme 1). The halide exchange reactions between **1** and an excess of the appropriate potassium halide were performed in a two-layer solvent system ($\text{H}_2\text{O}/\text{EtOH}/\text{CH}_2\text{Cl}_2$) and resulted in isolation of the dibromide **2** and

the diiodide **3** in almost quantitative yields. The analogous difluoride could not be isolated using a similar method even if a large excess of potassium or ammonium fluoride was used. Similar behavior has also been mentioned in the literature.^{1,13}

The ¹H NMR spectrum of **1** in CDCl_3 or CD_2Cl_2 at room temperature shows singlet signals for both the methylene and methyl protons and the corresponding doublet and triplet signals for the aromatic protons. This suggests equivalence of aliphatic protons from the two pendent arms. Low-temperature NMR spectra in CD_2Cl_2 , down to -55°C , showed no modification in the pattern of the resonance signals, thus indicating a high symmetry on the NMR time scale. The NMR spectra of the related dihalides **2** and **3** exhibit a similar pattern. A comparison of the ¹³C NMR spectra of compounds **1–3** revealed a notable high-field shift of the resonance signal corresponding to the carbon atom (C-1) directly attached to bismuth when chlorine is exchanged with bromine or iodine, respectively.

Crystal Structures of $2,6\text{-(Me}_2\text{NCH}_2)_2\text{C}_6\text{H}_3\text{BiX}_2$ (1–3). Crystal structures of the dihalides **1–3** were determined by X-ray diffraction from single crystals obtained by slow diffusion of *n*-hexane into a solution of the compound **1** in methylene chloride or by allowing hot, saturated DMSO solutions of compounds **2** and **3** to slowly reach room temperature. The solid-state molecular structures of all three compounds are very similar, as reflected by the selected molecular parameters given in Table 1. They exhibit a similar striking feature, i.e., a T-shaped geometry of the CBiX_2 core, with *trans* halogen atoms ($\text{Cl}(1)\text{-Bi}(1)\text{-Cl}(2)$ $173.73(3)^\circ$, $\text{Br}(1)\text{-Bi}(1)\text{-Br}(1a)$ $175.87(3)^\circ$, and $\text{I}(1)\text{-Bi}(1)\text{-I}(1a)$ $179.70(2)^\circ$) (see Figure 1 for the dichloride **1**).

Both nitrogen atoms of the organic ligand are strongly coordinated to bismuth in an almost *trans* arrangement ($\text{N}(1)\text{-Bi}(1)\text{-N}(2)$ $144.2(1)^\circ$ in **1**; $\text{N}(1)\text{-Bi}(1)\text{-N}(1a)$ $144.3(2)^\circ$ and $143.7(2)^\circ$ in **2** and **3**, respectively). This deviation from the ideal angle of 180° is due to the constraints imposed by the coordinated amine arms. The overall geometry at the bismuth center is distorted square pyramidal, with the carbon atom in the apical position. The T-shape arrangement of the CBiX_2 core together with the nitrogen dative bonds resembles a transition state in the *edge* inversion mechanism proposed by Dixon and Arduengo,¹⁴ and compounds **1–3** can be described as hypervalent 12-Bi-5 species.¹⁵

The *trans* Bi-halogen bond lengths in compounds **1–3** are considerably longer ($\text{Bi}(1)\text{-Cl}$ $2.701(1)$ and $2.706(1)$ Å in **1**; $\text{Bi}(1)\text{-Br}(1)$ $2.840(1)$ Å in **2**; $\text{Bi}(1)\text{-I}(1)$ $3.082(1)$ Å in **3**) than characteristic Bi-halogen covalent bonds ($\Sigma_{\text{cov}}(\text{Bi},\text{X})$ $2.51, 2.66$, and 2.85 Å for $\text{X} = \text{Cl}, \text{Br},$ and I , respectively),¹⁶ which is in agreement with the 3c-4e theory of the hypervalent bond formation. Similar values were found for the Bi-halogen distances in the polymeric structures of MeBiCl_2 ($2.741, 2.755$ Å),¹⁷ PhBiBr_2 ($2.880, 2.925$ Å),¹⁸ and MeBiI_2 ($3.086\text{--}3.128$

(13) Shimada S.; Yamazaki O.; Tanaka T.; Suzuki, Y.; Tanaka, M. *J. Organomet. Chem.* **2004**, *689*, 3012.

(14) Dixon, D. A.; Arduengo, A. J., III; Fukunaga, T. *J. Am. Chem. Soc.* **1986**, *108*, 2461. (b) Dixon, D. A.; Arduengo, A. J., III. *J. Chem. Phys.* **1987**, *91*, 3195.

(15) The *N-X-L* nomenclature system has been previously described: *N* valence shell electrons about a central atom X with *L* ligands. Perkins, C. W.; Martin, J. C.; Arduengo, A. J., III; Lau, W.; Alegria, A.; Kochi, K. *J. Am. Chem. Soc.* **1980**, *102*, 7753.

(16) Emsley, J. *Die Elemente*; Walter de Gruyter: Berlin, 1994.

(17) Althaus, H.; Breunig, H. J.; Lork, E. *Organometallics* **2001**, *20*, 586.

(18) Clegg, W.; Elsegood, M. R. J.; Errington, R. J.; Fisher, G. A.; Norman, N. C. *J. Mater. Chem.* **1994**, *4*, 891.

(12) (a) Peveling, K. Ph.D. Thesis, Universität Dortmund, Germany, 2003. (b) Dostál, L.; Cisařová, I.; Jambor, R.; Růžička, A.; Jirásko, R.; Holeček, J. *Organometallics* **2006**, *25*, 4366.

Table 1. Selected Bond Distances [Å] and Angles [deg] for Compounds 1–3

1		2 ^a		3 ^a	
Bi(1)–C(1)	2.224(4)	Bi(1)–C(1)	2.194(10)	Bi(1)–C(1)	2.216(7)
Bi(1)–Cl(1)	2.7012(11)	Bi(1)–Br(1)	2.8404(9)	Bi(1)–I(1)	3.0819(6)
Bi(1)–Cl(2)	2.7062(11)				
Bi(1)–N(1)	2.561(3)	Bi(1)–N(1)	2.566(5)	Bi(1)–N(1)	2.589(4)
Bi(1)–N(2)	2.570(4)				
N(1)–C(7)	1.482(5)	N(1)–C(5)	1.459(9)	N(1)–C(5)	1.484(7)
N(1)–C(8)	1.477(5)	N(1)–C(6)	1.460(8)	N(1)–C(6)	1.466(7)
N(1)–C(9)	1.471(5)	N(1)–C(7)	1.461(9)	N(1)–C(7)	1.481(6)
N(2)–C(10)	1.493(5)				
N(2)–C(11)	1.476(6)				
N(2)–C(12)	1.482(6)				
Cl(1)–Bi(1)–Cl(2)	173.73(3)	Br(1)–Bi(1)–Br(1a)	175.87(3)	I(1)–Bi(1)–I(1a)	179.70(2)
C(1)–Bi(1)–Cl(1)	87.11(10)	C(1)–Bi(1)–Br(1)	87.93(2)	C(1)–Bi(1)–I(1)	90.15(1)
C(1)–Bi(1)–Cl(2)	86.62(10)				
C(1)–Bi(1)–N(1)	72.14(13)	C(1)–Bi(1)–N(1)	72.17(12)	C(1)–Bi(1)–N(1)	71.83(9)
C(1)–Bi(1)–N(2)	72.04(14)				
N(1)–Bi(1)–N(2)	144.18(11)	N(1)–Bi(1)–N(1a)	144.3(2)	N(1)–Bi(1)–N(1a)	143.66(18)
N(1)–Bi(1)–Cl(1)	94.57(8)	N(1)–Bi(1)–Br(1)	95.53(11)	N(1)–Bi(1)–I(1)	95.52(9)
N(1)–Bi(1)–Cl(2)	83.79(8)	N(1)–Bi(1)–Br(1a)	83.20(12)	N(1)–Bi(1)–I(1a)	84.57(9)
N(2)–Bi(1)–Cl(1)	83.87(9)				
N(2)–Bi(1)–Cl(2)	93.90(9)				
C(7)–N(1)–C(8)	109.8(3)	C(5)–N(1)–C(6)	110.1(5)	C(5)–N(1)–C(6)	110.1(5)
C(7)–N(1)–C(9)	110.6(3)	C(5)–N(1)–C(7)	110.3(6)	C(5)–N(1)–C(7)	109.8(4)
C(8)–N(1)–C(9)	110.0(4)	C(6)–N(1)–C(7)	109.1(6)	C(6)–N(1)–C(7)	109.2(5)
Bi(1)–N(1)–C(7)	104.2(2)	Bi(1)–N(1)–C(5)	103.9(4)	Bi(1)–N(1)–C(5)	103.6(3)
Bi(1)–N(1)–C(8)	113.5(3)	Bi(1)–N(1)–C(6)	115.1(4)	Bi(1)–N(1)–C(6)	108.8(3)
Bi(1)–N(1)–C(9)	108.7(3)	Bi(1)–N(1)–C(7)	108.2(4)	Bi(1)–N(1)–C(7)	115.1(3)
C(10)–N(2)–C(11)	110.1(4)				
C(10)–N(2)–C(12)	110.4(4)				
C(11)–N(2)–C(12)	110.9(4)				
Bi(1)–N(2)–C(10)	104.2(3)				
Bi(1)–N(2)–C(11)	108.7(3)				
Bi(1)–N(2)–C(12)	112.4(3)				

^a Symmetry equivalent atoms (1–*x*, *y*, 1.5–*z*) for **2** and (1–*x*, *y*, 0.5–*z*) for **3** are given by “a”.

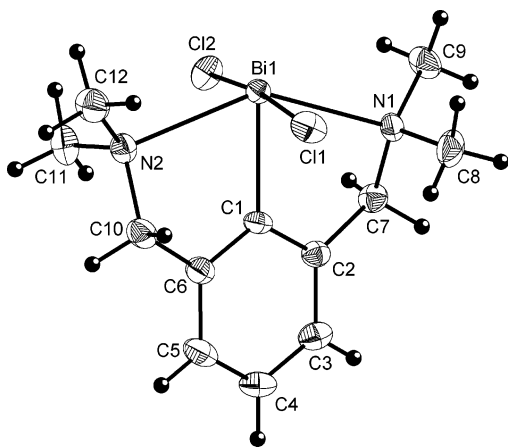


Figure 1. Molecular structure of the (*S*_{N1},*S*_{N2}) isomer of **1** (ORTEP drawing with 30% probability ellipsoids) with the labeling scheme for the atom positions.

Å),¹⁹ built on the basis of angular, slightly asymmetric Bi–X–Bi systems.

The Bi–N distances in compounds **1**–**3** are similar regardless of the nature of the halogen [**1**, 2.561(3), 2.570(4) Å; **2**, 2.566(5) Å; **3**, 2.589(4) Å] and lie between the sums of the corresponding covalent ($\Sigma_{\text{cov}}(\text{Bi},\text{N})$ 2.22 Å) and van der Waals radii ($\Sigma_{\text{vdW}}(\text{Bi},\text{N})$ 3.94 Å).¹⁶ These internal Bi–N interactions are much stronger than those observed in the related [2,6-(Me₂NCH₂)₂C₆H₃]Bi[C₆H₄{C(CF₃)₂O}-2] derivative (2.68(1), 2.86(1) Å), which however exhibits a pyramidal arrangement of the covalent bonds at bismuth.⁴ The (N,C,N)-coordination pattern

for the 2,6-(Me₂NCH₂)₂C₆H₃ ligand is well established in the transition metal chemistry.²⁰

As result of the intramolecular coordination of the nitrogen to the bismuth atom, two five-membered BiC₃N rings are formed. These rings are folded along the Bi(1)···C_{methylene} axis, with the nitrogen atom lying above the best plane defined by the residual BiC₃ system. This folding induces planar chirality (with the aromatic ring and the nitrogen atoms as chiral plane and pilot atoms, respectively)²¹ as described for other related compounds,²² and indeed compounds **1**–**3** crystallize as racemates, i.e., 1:1 mixtures of (*S*_{N1},*S*_{N2}) and (*R*_{N1},*R*_{N2}) isomers (with respect to the two chelate rings in a molecular unit). In the crystal both halogen atoms of a molecular unit are involved in Bi–X···Bi bridges, thus resulting in the formation of a doubly bridged polymeric chain that contains alternating (*S*_{N1},*S*_{N2}) and (*R*_{N1},*R*_{N2}) isomers in an *anti* arrangement regarding the axis of the polymer (see Figure 2 for the dibromide **2**). The intermolecular Bi···X interactions are weak. The corresponding contact

(20) (a) van Koten, G. *Pure Appl. Chem.* **1989**, *61*, 1681. (b) van Koten, G. *Pure Appl. Chem.* **1990**, *62*, 1155. (c) van Koten, G.; Terheijden, J.; van Beek, J. A. M.; Wehman-Ooyevaar, I. C. M.; Muller, F.; Stan, C. H. *Organometallics* **1990**, *9*, 903. (d) van Koten, G.; Jastrzebski, J. T. B. H.; Noh, J. G.; Spek, A. L.; Shoone, I. C. J. *Organomet. Chem.* **1978**, *148*, 233. (e) Yoshifuji, M.; Otoguro, A.; Toyota, K. *Bull. Chem. Soc. Jpn.* **1994**, *67*, 1503.

(21) *IUPAC Nomenclature of Organic Chemistry*; Pergamon Press: Oxford, 1979.

(22) (a) Opreş, L. M.; Silvestru, A.; Silvestru, C.; Breunig, H. J.; Lork, E. *Dalton Trans.* **2003**, 4367. (b) Bumbu, O.; Silvestru, C.; Gimeno, M. C.; Laguna, A. *J. Organomet. Chem.* **2004**, *689*, 1172. (c) Opreş, L. M.; Silvestru, A.; Silvestru, C.; Breunig, H. J.; Lork, E. *Dalton Trans.* **2004**, 3575. (d) Varga, R. A.; Silvestru, C.; Deleanu, C. *Appl. Organomet. Chem.* **2005**, *19*, 153. (e) Kulcsar, M.; Silvestru, A.; Silvestru, C.; Drake, J. E.; Macdonald, C. L. B.; Hursthouse, M. E.; Light, M. E. *J. Organomet. Chem.* **2005**, *690*, 3217. (f) Varga, R. A.; Rotar, A.; Schürmann, M.; Jurkschat K.; Silvestru, C. *Eur. J. Inorg. Chem.* **2006**, 1475.

(19) Wang, S.; Mitzi, D. B.; Landrum, G. A.; Genin, H.; Hoffmann, R. *J. Am. Chem. Soc.* **1997**, *119*, 724.

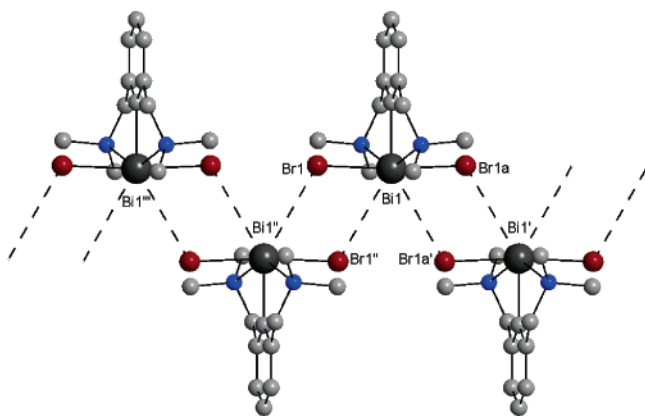


Figure 2. View along *a*-axis of the supramolecular association based on intermolecular bismuth–bromine interactions in the crystal of **2** [symmetry equivalent atoms (*x*, 1−*y*, −0.5+*z*) and (1−*x*, 1−*y*, 2−*z*) for Br1a' and Br1'', respectively]. Hydrogen atoms are omitted for clarity.

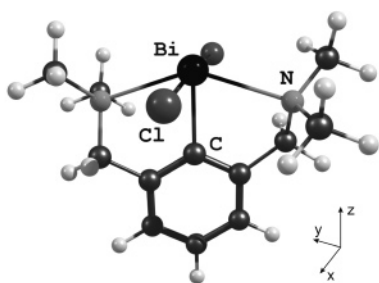


Figure 3. Optimized structure of [2,6-(Me₂NCH₂)₂C₆H₃]BiCl₂, **1**. Selected distances (Å) and angles (deg): Bi–Cl 2.67, Bi–N 2.54, Bi–C 2.22; N–Bi–N 143.8, Cl–Bi–Cl 175.4.

distances [**1**, Bi(1)⋯Cl(1') 3.620(1) Å, Bi(1)⋯Cl(2'') 3.545(1) Å; **2**, Bi(1)⋯Br(1'') 3.818(1) Å; **2**, Bi(1)⋯I(1') 4.021(1) Å] are shorter than the sums of the corresponding van der Waals radii ($\sum_{vdW}(Bi,X)$ 4.21, 4.35, and 4.55 Å for X = Cl, Br, and I, respectively).¹⁶

DFT Calculations. The electronic structure of **1** was analyzed by density functional theory (DFT) calculations to gain insight into the nature of bonding and to clarify why in this type of complexes a square pyramidal geometry is favored over a trigonal pyramidal geometry. The structure of **1** was optimized at the DFT level of theory without symmetry restraints, but the optimized structure was very close to *C*₂ symmetry (Figure 3). Hence the orbitals are labeled either a or b corresponding to the irreducible representations of this point group. The calculated Bi–Cl (2.67 Å) and Bi–N (2.54 Å) distances are in good agreement with the corresponding experimental distances determined by single-crystal X-ray diffractions (Bi–Cl 2.7012(11) and 2.7062(11) Å; Bi–N 2.561(3) and 2.570(4) Å). Also the other calculated geometrical parameters are in good agreement with the experimental data.

The bonding in **1** was analyzed by considering the interaction of the bismuth atomic orbitals with those of the ligands. This shows no hybridization of the Bi *s* and *p* orbitals. For the bonding, the bismuth atom uses only its 6*p* orbitals, while the 6*s* orbital remains nonbonding. The Bi–Cl bonding is realized through in-phase combination of the Bi *p_x* orbital with the *p_x* orbitals of both chlorine atoms, leading to a bonding molecular orbital (MO) (21b in Figure 4). Similarly the Bi *p_y* orbital mixes mainly with the *p_y* orbitals of the two nitrogen atoms of the −CH₂NMe₂ pendent arms to give a Bi–N bonding MO (22b). The Bi–C bonding is realized mainly through the Bi *p_z* orbital and the *ipso* carbon *p_z* orbital of the aromatic ring (23a). The

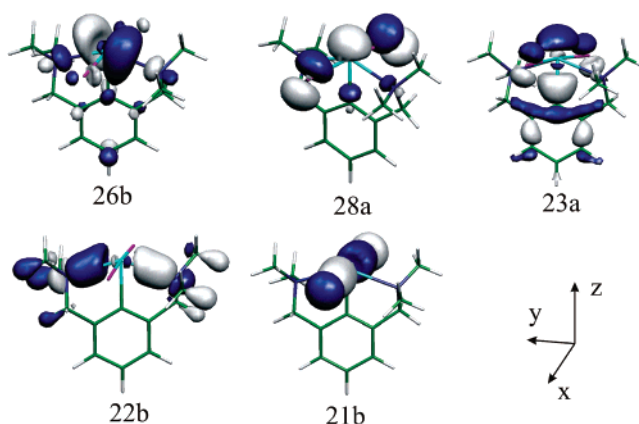


Figure 4. Isosurfaces of selected molecular orbitals of **1**. The orbitals are labeled in the *C*₂ symmetry.

out-of-phase combination of the Bi *p_y* and N *p_y* orbitals forms the LUMO (26b), while the HOMO (28a) is formed by the lone pairs of the chlorine atoms containing relatively small Bi contribution (*s* and *p_z*). The high stability of **1** is also confirmed by the large HOMO–LUMO gap (3.62 eV).

The analysis of the Hirshfeld charge distributions shows that **1** is relatively strongly polarized. The chlorine atoms are clearly negatively charged (−0.32), the nitrogen atoms are slightly (−0.03) negatively charged, while the bismuth atom is positively charged (0.49).

Considering the orbital interactions described above and the charge distribution, overall the bonding in **1** is excellently described by two three-center–four-electron bonds (Bi–Cl and Bi–N) and a two-center–two-electron bond (Bi–C).

To quantify the stabilization obtained by the coordination of the pendent −CH₂NMe₂ arms to the Bi, the relative energies of different isomers of **1** (Figure 5) were calculated. In the structure of lowest energy both nitrogen atoms are coordinated to bismuth (**1**), which was also observed experimentally in the crystal structure. To evaluate the amount of stabilization of one N→Bi interaction, one pendent −CH₂NMe₂ arm was rotated 180° around the C–C(Ph) bond in such a way that the nitrogen is situated far away from the bismuth atom and hence one N→Bi interaction is eliminated. Geometry optimization without any constraints leads to a geometry with a bent Cl–Bi–Cl unit (**1a**), which is 17.61 kcal·mol^{−1} higher in energy than **1**. Constraining in **1a** the Cl–Bi–Cl angle to linearity (**1b**) leads to only a slight increase in energy (0.22 kcal·mol^{−1}) compared to **1a**. The elimination of the second N→Bi interaction in **1a** gives rise to an increase in energy of 9.76 kcal·mol^{−1} for **1c** compared to **1a**. If the Cl–Bi–Cl angle is enforced to linearity and both bismuth–nitrogen interactions are cancelled (**1d**), then the structure increases considerably in energy. Overall the two N→Bi coordinations of the two −CH₂NMe₂ pendent arms stabilize the square pyramidal geometry by 38.40 kcal·mol^{−1}.

The analysis of the calculated relative energies of different isomers of **1** shows that only one N→Bi coordination is not enough to clearly stabilize the T-shaped versus the trigonal pyramidal geometry of the CBiCl₂ system. However the energy difference between the two geometries is fairly small. The T-shaped geometry of the CBiCl₂ unit is strongly stabilized by the second N→Bi coordination. The low energy difference between the isomers **1a** and **1b** and the high energy difference between **1** and **1a** show that the stabilization of the square pyramidal geometry of bismuth is electronic rather than steric in nature.

The structure of **1** can also be rationalized by means of the valence shell electron pair repulsion (VSEPR) theory. According

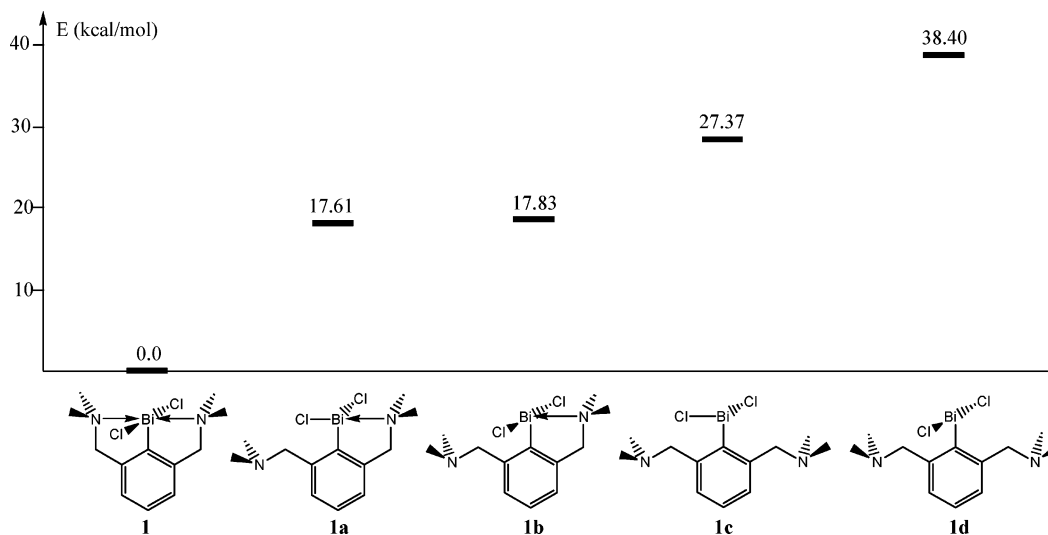


Figure 5. Calculated relative energies of different isomers of [2,6-(Me₂NCH₂)₂C₆H₃]BiCl₂, **1**.

to this, the Bi atom in **1** has six electron pairs and the structure is predicted to be based on an octahedron with one lone pair, hence the square pyramidal shape. However in post-transition elements such as bismuth the lone pair is not always stereochemically active. This is confirmed by our calculations, which show that the lone pair of electrons is situated in the energetically low lying 6s atomic orbital of the bismuth. After removing one –CH₂NMe₂ pendent arm, the bismuth atom will have five electron pairs; hence a geometry based on a trigonal bipyramid with a lone pair in equatorial position would be expected. That is in agreement with the calculated structures for **1a** and **1b**; however the close to 90° angles are smaller than those expected from the VSEPR model. After removing the second –CH₂NMe₂ pendent arm, the bismuth atom will have four electron pairs, and a distorted tetrahedral geometry with one electron pair would be expected. The optimization of the geometry of **1c** confirms that, however, the bond angles are close to 90°. We believe that these values are better explained by the absence of hybridization of the bismuth atom than by the VSEPR model.

Synthesis and Structural Characterization of [2,6-(Me₂NCH₂)₂C₆H₃](Me)BiI (4**).** In order to obtain a chiral compound, the dichloride **1** was reacted with methylmagnesium iodide in a 1:1 molar ratio (Scheme 1). The monoiodide [2,6-(Me₂NCH₂)₂C₆H₃]Bi(Me)I (**4**) was obtained due to the exchange of chlorine with iodine from the resulting inorganic magnesium salt. The diiodide **3** was also isolated as a byproduct of this reaction.

The ¹H NMR spectrum of **4** in CDCl₃, at room temperature, showed two singlet signals for the methyl groups attached to bismuth and nitrogen atoms, respectively, and an AB system for methylene protons. The aromatic protons appeared as an unresolved, broad signal. When the ¹H NMR spectrum of **4** was recorded at low temperature, a broadening of the resonance for the methyl groups attached to the nitrogen atoms was observed until 5 °C. At –10 °C this signal was completely resolved into a doublet (see Supporting Information), indicating that both nitrogen atoms are coordinated to the metal center and the molecule is frozen to a structure resembling that found in the solid state (see subsequent discussion). This process corresponds to the dissociation–recoordination between the nitrogen atoms and the bismuth atom, with inversion at a three-coordinated nitrogen atom and rotation around the (H₂)C–N bond. The activation energy of this process was estimated to be ΔG[‡]–

(CDCl₃) = 14 kcal mol^{–1} (T_c = 5 °C).²³ Similar activation energies for the dissociation of either one of the Bi–N bonds (12.3 kcal mol^{–1} at –5 °C, in toluene-*d*₈) were estimated for [2,6-(Me₂NCH₂)₂C₆H₃]Bi[C₆H₄{C(CF₃)₂O}–2]⁴ or for the related [2-(Me₂NCH₂)C₆H₄]BiCl[(SPPPh₂)₂N] (14.7 kcal mol^{–1} at 25 °C, in CDCl₃).^{10b}

In the crystal of **4** discrete diorganobismuth(III) iodide molecules cannot be distinguished; instead there is a supramolecular zigzag chain in which alternating (R_{N1},R_{N2})- and (S_{N1},S_{N2})-[2,6-(Me₂NCH₂)₂C₆H₃]Bi(Me)] units are bridged by iodine (Figure 6). Selected molecular parameters are given in Table 2. The bent Bi⋯I⋯Bi bridges (157.19(2)°) are almost symmetric, and the metal–halogen distances (Bi(1)–I(1′) 3.924(1) Å, Bi(1)–I(1′′) 4.022(1) Å) indicate weak interactions similar to the intermolecular Bi⋯I interaction (3.990 Å), leading to the chain polymeric association observed in the solid state for Ar(4-ClC₆H₄)BiI (Ar = 2-[(R)-1-(dimethylamino)ethyl]ferrocenyl) (cf. the sum of the van der Waals radii, Σ_{vdW}(Bi,I) 4.55 Å).¹⁶

Both nitrogen atoms of the ligand are strongly coordinated to bismuth in a fashion similar to that observed for the dihalides **1–3** (*trans* N(1)–Bi(1)–N(2) 144.9(3)°). The strength of these interactions (Bi(1)–N(1) 2.555(8) Å, Bi(1)–N(2) 2.540(8) Å) is also similar to those found in compounds **1–3**. If the weak Bi⋯I interactions are neglected, the coordination of the metal center is distorted *ψ*-trigonal bipyramidal (“seesaw”), with the nitrogen atoms in apical positions. The vectors of the Bi⋯I interactions are directed almost *trans* to the carbon atoms (C(1)–Bi(1)⋯I(1′) 147.6(2)°, C(13)–Bi(1)⋯I(1′′) 168.9(3)°), thus completing a distorted octahedral environment around the bismuth atom.

Synthesis and Structural Characterization of [2,6-(Me₂NCH₂)₂C₆H₃]BiCl (5**).** By reacting [2,6-(Me₂NCH₂)₂C₆H₃]–Li with BiCl₃ in a 2:1 ratio, compound **5** was obtained (Scheme 1).^{10e} The ¹H NMR of the precipitate initially isolated from the reaction mixture indicated contamination with a small amount of **1**. Crystals of compound **5** could be grown only by rapid removal of the solvent from an ethereal solution. Only crystals of the side product **1** were obtained after slow evaporation from solutions of **5** in various solvents.

The NMR spectra of a fresh solution of **5** in CDCl₃, at room temperature, are consistent with equivalent organic groups

(23) Friebolin, H. *Basic One- and Two-Dimensional NMR Spectroscopy*, 3rd ed.; Wiley-VCH Verlag GmbH: Weinheim, 1998; p 301.

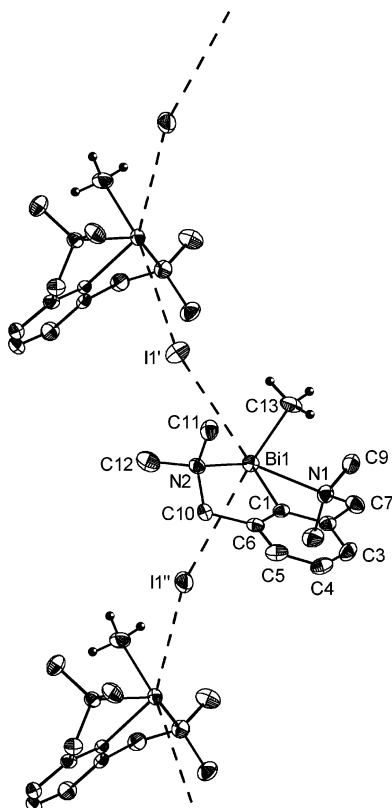


Figure 6. Part of the polymeric chain of **4** (ORTEP drawing with 30% probability ellipsoids) with the labeling scheme for the atom positions [symmetry equivalent atoms $(1-x, -0.5+y, 1.5-z)$ and $(0.5+x, y, 1.5-z)$ for $I1'$ and $I1''$, respectively]. Hydrogen atoms, less those of the methyl group attached to the metal, have been omitted for clarity.

Table 2. Selected Bond Distances [Å] and Angles [deg] for Compound 4^a

Bi(1)–C(1)	2.204(8)	Bi(1)–C(13)	2.224(10)
Bi(1)–I(1')	3.924(1)	Bi(1)–I(1'')	4.022(1)
Bi(1)–N(1)	2.555(8)	Bi(1)–N(2)	2.540(8)
N(1)–C(7)	1.472(12)	N(2)–C(10)	1.482(12)
N(1)–C(8)	1.474(13)	N(2)–C(11)	1.482(12)
N(1)–C(9)	1.475(13)	N(2)–C(12)	1.480(12)
C(1)–Bi(1)–C(13)	91.2(4)	N(1)–Bi(1)–N(2)	144.9(3)
N(1)–Bi(1)–C(1)	71.9(3)	N(2)–Bi(1)–C(1)	73.0(3)
N(1)–Bi(1)–C(13)	93.1(4)	N(2)–Bi(1)–C(13)	87.9(4)
C(7)–N(1)–C(8)	110.1(8)	C(10)–N(2)–C(11)	109.5(7)
C(7)–N(1)–C(9)	109.6(8)	C(10)–N(2)–C(12)	109.0(8)
C(8)–N(1)–C(9)	110.5(8)	C(11)–N(2)–C(12)	109.2(8)
Bi(1)–N(1)–C(7)	104.2(5)	Bi(1)–N(2)–C(10)	104.9(5)
Bi(1)–N(1)–C(8)	111.4(6)	Bi(1)–N(2)–C(11)	106.1(5)
Bi(1)–N(1)–C(9)	111.1(6)	Bi(1)–N(2)–C(12)	117.8(6)

^a Symmetry equivalent atoms $(1-x, -0.5+y, 1.5-z)$ and $(0.5+x, y, 1.5-z)$ for $I1'$ and $I1''$, respectively.

attached to bismuth. The broad singlet resonances observed for the methyl and methylene protons, respectively, suggest a fluxional behavior. Time-dependent ¹H NMR spectra starting from crystals of compound **5** proved that a disproportionation process to **1** and R₃Bi occurs in CDCl₃ solution. The molar ratio between the signals corresponding to the methylene protons of compounds **1** and **5** increases during 2 days from 1:340 to 1:13.

A single-crystal X-ray diffraction study revealed that in the molecules of **5** only three of four available nitrogen atoms coordinate to bismuth. In contrast to the dihalides **1–3** and compound **4**, the ligand that exhibits a (N,C,N)-coordination pattern in **5** has both nitrogen atoms on the same side of the plane of the aromatic ring. The other organic group acts as a

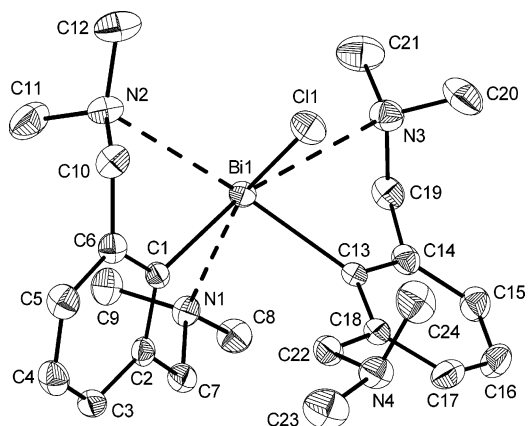


Figure 7. Molecular structure of the $(R_{N1}, S_{N2})(S_{N3})$ isomer of **5** (ORTEP drawing with 30% probability ellipsoids) with the labeling scheme for the atom positions. Hydrogen atoms have been omitted for clarity.

Table 3. Selected Bond Distances [Å] and Angles [deg] for Compound 5

Bi(1)–C(1)	2.278(4)	Bi(1)–C(13)	2.301(4)
Bi(1)–Cl(1)	2.6086(13)		
Bi(1)–N(1)	2.699(3)		
Bi(1)–N(2)	3.070(3)	Bi(1)–N(3)	3.118(3)
N(1)–C(7)	1.478(5)	N(3)–C(19)	1.449(5)
N(1)–C(8)	1.469(5)	N(3)–C(20)	1.454(6)
N(1)–C(9)	1.460(5)	N(3)–C(21)	1.455(6)
N(2)–C(10)	1.457(5)	N(4)–C(22)	1.455(5)
N(2)–C(11)	1.448(6)	N(4)–C(23)	1.447(6)
N(2)–C(12)	1.451(6)	N(4)–C(24)	1.453(6)
C(1)–Bi(1)–C(13)	100.13(14)	N(1)–Bi(1)–C(1)	69.64(12)
C(1)–Bi(1)–Cl(1)	96.42(11)	N(1)–Bi(1)–C(13)	81.03(12)
C(13)–Bi(1)–Cl(1)	85.95(10)	N(1)–Bi(1)–Cl(1)	158.72(8)
N(2)–Bi(1)–C(13)	152.66(11)	N(3)–Bi(1)–C(1)	166.82(10)
N(2)–Bi(1)–C(1)	64.08(10)	N(3)–Bi(1)–C(13)	66.70(10)
N(2)–Bi(1)–Cl(1)	74.60(8)	N(3)–Bi(1)–Cl(1)	82.78(8)
N(2)–Bi(1)–N(1)	110.94(10)	N(3)–Bi(1)–N(1)	107.06(9)
N(2)–Bi(1)–N(3)	127.71(9)		
C(7)–N(1)–C(8)	108.9(3)	C(19)–N(3)–C(20)	110.3(4)
C(7)–N(1)–C(9)	111.8(3)	C(19)–N(3)–C(21)	109.7(4)
C(8)–N(1)–C(9)	109.5(3)	C(20)–N(3)–C(21)	110.2(4)
Bi(1)–N(1)–C(7)	100.3(2)	Bi(1)–N(3)–C(19)	81.3(2)
Bi(1)–N(1)–C(8)	118.8(3)	Bi(1)–N(3)–C(20)	125.3(3)
Bi(1)–N(1)–C(9)	107.2(3)	Bi(1)–N(3)–C(21)	111.7(2)
C(10)–N(2)–C(11)	111.4(4)	C(22)–N(4)–C(23)	111.7(4)
C(10)–N(2)–C(12)	111.5(4)	C(22)–N(4)–C(24)	111.0(4)
C(11)–N(2)–C(12)	110.6(4)	C(23)–N(4)–C(24)	111.8(4)
Bi(1)–N(2)–C(10)	93.0(2)		
Bi(1)–N(2)–C(11)	112.4(3)		
Bi(1)–N(2)–C(12)	116.8(3)		

(C,N) ligand, with the nitrogen of the second arm twisted far from the metal center. The compound crystallizes as a 1:1 mixture of $(R_{N1}, S_{N2})(S_{N3})$ and $(S_{N1}, R_{N2})(R_{N3})$ isomers, the former being depicted in Figure 7. Selected molecular parameters are given in Table 3.

The Bi–N vectors lie almost *trans* to a normal covalent bond: N(1)–Bi(1)–Cl(1) 158.72(8)°, N(2)–Bi(1)–C(13) 152.66(11)°, and N(3)–Bi(1)–C(1) 166.82(10)°. The Bi(1)–N(1) and the Bi(1)–Cl(1) bonds are *trans* to each other and are weaker (2.699(3) Å) and stronger (2.6086(13) Å), respectively, with respect to the analogous *trans*-N–Bi–Cl system in the related $[2-(\text{Me}_2\text{NCH}_2)\text{C}_6\text{H}_4]_2\text{BiCl}$ (Bi–N 2.570(5) Å, Bi–Cl 2.667(2) Å).⁸ The other two intramolecular bismuth–nitrogen interactions are considerably weaker (Bi(1)–N(2) 3.070(3) Å, Bi(1)–N(3) 3.118(3) Å), but still shorter than the sum of the van der Waals radii for Bi and N atoms. A similar value was also found for the second intramolecular Bi–N interaction (3.047(5) Å) in $[2-(\text{Me}_2\text{NCH}_2)\text{C}_6\text{H}_4]_2\text{BiCl}$,⁸ while the Bi–N interactions in the

Table 4. Data Collection and Structure Refinement Details for Compounds 1–5

	1	2	3	4	5
chemical formula	C ₁₂ H ₁₉ BiCl ₂ N ₂	C ₁₂ H ₁₉ BiBr ₂ N ₂	C ₁₂ H ₁₉ BiI ₂ N ₂	C ₁₃ H ₂₂ BiN ₂	C ₂₄ H ₃₈ BiClN ₄
cryst habit	colorless block	colorless block	yellow block	colorless block	colorless block
cryst size [mm]	0.29 × 0.22 × 0.18	0.43 × 0.17 × 0.12	0.28 × 0.17 × 0.13	0.25 × 0.19 × 0.17	0.24 × 0.22 × 0.13
cryst syst	triclinic	orthorhombic	orthorhombic	orthorhombic	monoclinic
space group	<i>P</i> $\bar{1}$	<i>Pbcn</i>	<i>Pbcn</i>	<i>Pbca</i>	<i>P</i> $\bar{1}$ 21/ <i>n</i>
<i>a</i> [Å]	8.2936(7)	16.177(4)	16.278(3)	11.9840(17)	9.9668(7)
<i>b</i> [Å]	10.2996(8)	11.491(3)	11.848(2)	13.3474(19)	17.2075(12)
<i>c</i> [Å]	10.3432(8)	8.4265(19)	8.8883(16)	20.537(3)	15.5319(11)
α [deg]	66.9920(10)	90	90	90	90
β [deg]	75.1250(10)	90	90	90	94.7380(10)
γ [deg]	81.9120(10)	90	90	90	90
<i>U</i> [Å ³]	785.18(11)	1566.4(7)	1714.2(5)	3284.9(8)	2654.7(3)
<i>Z</i>	2	4	4	8	4
<i>D</i> _c [g cm ⁻³]	1.993	2.375	2.534	2.193	1.569
<i>M</i>	471.17	560.09	654.07	542.21	627.01
<i>F</i> (000)	444	1032	1176	2000	1240
<i>T</i> [°C]	24	24	24	24	24
2 θ _{max} [deg]	56.26	52.74	52.74	52.74	52.74
μ (Mo K α) [mm ⁻¹]	11.550	16.341	13.872	12.599	6.759
no. of reflns measd	6764	11 626	12 755	24 755	21 075
no. of unique reflns	3496	1609	1761	3356	5423
<i>R</i> _{int}	0.0253	0.0673	0.0406	0.0507	0.0459
<i>R</i> ^a (<i>I</i> > 2 σ (<i>I</i>))	0.0238	0.0340	0.0245	0.0483	0.0310
<i>wR</i> ^b (<i>F</i> ² , all reflns)	0.0516	0.0868	0.0482	0.0968	0.0596
no. of params	158	81	82	159	279
no. of restraints	0	0	0	0	0
<i>S</i> ^c	1.021	1.111	1.138	1.159	1.043
$\Delta\rho$, max., min. [e Å ⁻³]	0.965, -1.211	1.247, -1.551	0.954, -1.128	2.805, -1.318	0.993, -0.503

^a $R_1 = \sum ||F_o| - |F_c|| / \sum |F_o|$. ^b $wR_2 = \{ \sum [w(F_o^2 - F_c^2)^2] / \sum [w(F_o^2)^2] \}^{1/2}$. $w = 1 / [\sigma^2(F_o^2) + (w_1P)^2 + w_2P]$, where $P = [2F_c^2 + \text{Max}(F_o^2)]/3$. ^c $\text{Goof} = S = \{ \sum [w(F_o^2 - F_c^2)^2] / (n - p) \}^{1/2}$, where n is the number of reflections and p is the total number of parameters refined.

dibismuthane [2,6-(Me₂NCH₂)₂C₆H₃]₄Bi₂ are even weaker (range 3.183(11)–3.370(10) Å).^{10e} If all three metal–nitrogen interactions are taken into account, a distorted octahedral (*N,C,N*)(*C,N*)BiX core can be considered, with the deviations of the bond angles at the metal atom from the ideal values mainly due to the constraints imposed by the coordinated amine arms (Table 3).

In the crystal of **5** the discrete monomeric molecular units are separated by normal van der Waals distances between heavy atoms. However, a closer inspection of the crystal structure revealed that between the halogen atom and the *para* hydrogen atom of the (*N,C,N*) ligand of a neighboring molecule a weak intermolecular interaction is established [Cl⋯H_{aryl} 2.958 Å, at the limit of a van der Waals contact, $\sum_{\text{vdW}}(\text{Cl,H})$ ca. 3.0 Å].¹⁶ This results in a supramolecular chain polymer, with alternating (*R*_{N1},*S*_{N2})(*S*_{N3}) and (*S*_{N1},*R*_{N2})(*R*_{N3}) molecular units.

Experimental Section

General Procedures. 1,3-Bis[(dimethylamino)methyl]benzene, 1,3-(Me₂NCH₂)₂C₆H₄,⁴ and the monochloride [2,6-(Me₂NCH₂)₂C₆H₃]₂-BiCl (**5**),^{10e} were obtained according to reported literature methods. Details for the preparation and spectroscopic characterization of the dichloride [2,6-(Me₂NCH₂)₂C₆H₃]₂BiCl₂ (**1**) (see also ref 9) are included in the Supporting Information. Bismuth trichloride was sublimated in vacuum and kept under argon. All other reagents were obtained from Aldrich or Merck and were used as received. All the syntheses were carried out under an argon atmosphere using dried solvents, distilled under argon prior to use.

Instrumentation. Elemental analyses were carried out with a Perkin-Elmer 2400 apparatus. Melting points were measured on an Electrothermal 9200 apparatus and are not corrected. Mass spectra were recorded on Finnigan MAT 8200 (EI, CI) or Bruker Esquire LC (ESI) instruments. ¹H, ¹³C, and 2D NMR spectra were recorded on Bruker Avance DPX 200 and 360, DRX 400, or DRX 600 instruments in CDCl₃ solutions, at room temperature. Variable-

temperature ¹H NMR spectra were recorded on a Bruker Avance DPX 200 instrument. Chemical shifts are reported in δ units (ppm) relative to the residual peak of the deuterated solvent (ref CHCl₃: ¹H 7.26, ¹³C 77.0 ppm).

Synthesis of [2,6-(Me₂NCH₂)₂C₆H₃]₂BiBr₂ (2**).** A solution of compound **1** (1.0 g, 2.1 mmol) in CH₂Cl₂ (20 mL) was vigorously stirred for 48 h with a solution of KBr (1.0 g, 8.4 mmol) in EtOH (25 mL) and distilled water (15 mL). Additional distilled water (50 mL) was then added, and the colorless organic phase was removed with a syringe. The aqueous phase was washed with CH₂-Cl₂ (25 mL). The organic phases were washed with distilled water (2 × 25 mL) and then dried over anhydrous Na₂SO₄. The solution was filtered off and the solvent removed in vacuum. The remaining white powder was washed with hexane (4 × 10 mL) and then dried in vacuum to give compound **2**. Yield: 1.04 g (88%), mp 261 °C (dec). Anal. Calcd for C₁₂H₁₉BiBr₂N₂ (MW 560.08): C, 25.73; H, 3.42; N, 5.00. Found: C, 25.55; H, 3.34; N, 5.12. ¹H NMR (360 MHz, CDCl₃): 2.98 (12H, s, CH₃), 4.50 (4H, s, CH₂), 7.51 (1H, t, Ar-H4, ³J_{HH} = 7.5 Hz), 7.73 (2H, d, Ar-H3,5, ³J_{HH} = 7.5 Hz). ¹³C NMR (90 MHz, CDCl₃): 48.42 (s, CH₃), 69.24 (s, CH₂), 128.39 (s, Ar-C3,5), 129.52 (s, Ar-C4), 151.84 (s, Ar-C2,6), 204.93 (s, Ar-C1). Mass spectrum (EI, 70 eV): *m/z* (relative intensity, %) 480 (100) [M⁺ - Br], 400 (9) [R_{Bi}⁺], 209 (10) [Bi⁺], 191 (71) [R⁺] [R = 2,6-(Me₂NCH₂)₂C₆H₃].

Synthesis of [2,6-(Me₂NCH₂)₂C₆H₃]₂BiI₂ (3**).** A similar procedure to that for compound **2** was used, with compound **1** (1.0 g, 2.1 mmol) in CH₂Cl₂ (40 mL) and KI (1.7 g, 10.2 mmol) in EtOH (25 mL) and distilled water (15 mL). Compound **3** was isolated as a yellow powder. Yield: 1.26 g (91%), mp 203 °C (dec). Anal. Calcd for C₁₂H₁₉BiI₂N₂ (MW 654.09): C, 22.04; H, 2.93; N, 4.28. Found: C, 21.83; H, 2.78; N, 4.05. ¹H NMR (360 MHz, CDCl₃): 3.12 (12H, s, CH₃), 4.55 (4H, s, CH₂), 7.56 (1H, t, Ar-H4, ³J_{HH} = 7.5 Hz), 7.75 (2H, d, Ar-H3,5, ³J_{HH} = 7.5 Hz). ¹³C NMR (90 MHz, CDCl₃): 50.95 (s, CH₃), 71.31 (s, CH₂), 128.65 (s, Ar-C3,5), 129.73 (s, Ar-C4), 152.46 (s, Ar-C2,6), 197.91 (s, Ar-C1). Mass spectrum (EI, 70 eV): *m/z* (relative intensity, %) 527 (100) [M⁺ - I], 400

(29) [RBi⁺], 209 (7) [Bi⁺], 191 (34) [R⁺] [R = 2,6-(Me₂NCH₂)₂C₆H₃].

Synthesis of [2,6-(Me₂NCH₂)₂C₆H₃](Me)BiI (4). A solution of MeMgI [Mg turnings (0.103 g, 4.24 mmol) and MeI (0.603 g, 4.24 mmol)] in Et₂O (25 mL) was added dropwise to a suspension of compound **1** (2.0 g, 4.24 mmol) in Et₂O. The reaction mixture was stirred at room temperature for 10 h to give a yellow, ethereal solution and a yellow precipitate. Distilled water (80 mL) was then added, and the whole mixture was filtered through a glass frit to give a yellow solid and a yellow organic phase. The yellow precipitate was investigated and turned out to be compound **3**. The yellow organic phase was separated and dried over anhydrous Na₂SO₄. Upon removal of the solvent, compound **4** was obtained as pale yellow powder. Yield: 0.77 g (34%), mp 210 °C. Anal. Calcd for C₁₃H₂₂BiIN₂ (MW 542.22): C, 28.80; H, 4.09; N, 5.17. Found: C, 28.63; H, 3.96; N, 5.34. ¹H NMR (200 MHz, CDCl₃, 20 °C): 1.68 (3H, s, Bi-CH₃), 2.81 (12H, s, N-CH₃), AB spin system with A at 3.90 and B at 4.06 ppm (4H, CH₂, ²J_{HH} = 14.6 Hz), 7.44 (3H, s, br, C₆H₃). ¹H NMR (200 MHz, CDCl₃, -10 °C): 1.64 (3H, s, Bi-CH₃), 2.72 (6H, s, N-CH₃), 2.85 (6H, s, N-CH₃), AB spin system with A at 3.89 and B at 4.04 ppm (4H, CH₂, ²J_{HH} = 14.6 Hz), 7.42 (3H, s, br, C₆H₃). ¹³C NMR (50 MHz, CDCl₃, 20 °C): 38.41 (s, Bi-CH₃), 47.77 (s, N-CH₃), 68.85 (s, CH₂), 127.26 (s, Ar-C3,5), 128.71 (s, Ar-C4), 148.40 (s, Ar-C2,6), 181.18 (s, Ar-C1). Mass spectrum (EI, 70 eV): *m/z* (relative intensity, %) 527 (57) [M⁺ - Me], 481 (17) [M⁺ - Me₃N], 415 (100) [M⁺ - I], 400 (82) [RBi⁺], 209 (13) [Bi⁺], 191 (64) [R⁺]. Mass spectrum (ESI, positive, MeOH/CH₂Cl₂): *m/z* (relative intensity, %) 543 [M⁺], 527 [M⁺ - Me], 415 [M⁺ - I], 400 [RBi⁺], 191 [R⁺]. Mass spectrum (ESI, negative, MeOH/CH₂Cl₂): *m/z* (relative intensity, %) 209 [Bi⁻], 127 [I⁻].

Crystallography. Colorless crystals of compounds **1** were grown by slow diffusion, using CH₂Cl₂/hexane systems. Colorless crystals of compound **2** and yellow crystals of compound **3** were grown by cooling hot, saturated DMSO solutions. Pale yellow crystals of compound **4** were grown by slow diffusion using a CH₂Cl₂/petroleum ether system. Colorless crystals of compound **5** were obtained by fast removal of the solvent from an Et₂O solution. The crystals were attached to a cryo loop. Data were collected at room temperature on a Bruker SMART APEX diffractometer, using graphite-monochromated Mo K α radiation (λ = 0.71073 Å). Scan type ω and ϕ . Absorption corrections: multiscan. The structures were solved by direct methods and refined on *F*² using the program SHELXL-97.²⁴ All non-hydrogen atoms were anisotropically refined. The hydrogen atoms were refined with a riding model and a mutual isotropic thermal parameter. Further details on the data collection and refinement methods can be found in Table 4. The drawings were created with the Diamond program.²⁵ CCDC-619307–619311 contain the supplementary crystallographic data for this paper. These data can be obtained free of charge via www.ccdc.cam.ac.uk/conts/retrieving.html (or from the Cambridge

(24) Sheldrick, G. M. *SHELX-97*; Universität Göttingen: Germany, 1997.

(25) *DIAMOND—Visual Crystal Structure Information System*; Crystal Impact: Postfach 1251, D-53002 Bonn, Germany, 2001.

Crystallographic Data Centre, 12 Union Road, Cambridge CB2 1EZ, UK; fax: (+44) 1223-336-033; ore-mail: deposit@ccdc.cam.ac.uk).

Computational Details for DFT Calculations. Density functional calculations were carried out using the Amsterdam Density Functional program suite ADF 2005.01.²⁶ Scalar relativistic corrections were included via the ZORA method for all calculations.²⁷ The generalized gradient approximation was employed, using the local density approximation of Vosko, Wilk, and Nusair²⁸ together with the nonlocal exchange correction by Becke²⁹ and nonlocal correlation corrections by Perdew.³⁰ TZP basis sets were used with triple- ζ accuracy sets of Slater-type orbitals and two polarization functions added to the main group atoms. The cores of the atoms were frozen up to 1p for C and N, 2p for Cl, and 5p for Bi. All quoted electronic structure data have gradient corrections applied after the SCF cycles. For comparing the relative energies of the different isomers the SCF energies were used.

Acknowledgment. Financial support from National University Research Council (CNCSIS, Romania; Research Project Nos. A-709/2006 and TD-100/2006) and the Ministry of Education and Research of Romania (Excellency Research Program, project CEx-05-D11-16/2005) is greatly appreciated. We thank Universitat Bremen for providing research facilities and financial support during short-term research stays. We also thank the National Center for X-Ray Diffraction and Dr. Richard Varga (“Babes-Bolyai” University, Cluj-Napoca, Romania) for the support in the solid-state structure determinations. We thank the Oxford Supercomputing Centre for facilities and support. G.B. thanks the Alexander von Humboldt Foundation for a Feodor Lynen Fellowship.

Supporting Information Available: Details of the synthesis and spectroscopic characterization of compounds **1** and **5**; X-ray crystallographic data in CIF format for **1–5**; Cartesian coordinates of the modeled structures of complexes **1–1d**; figures representing the molecular structures of compounds **2** and **3**, as well as the supramolecular architectures in the crystals of compounds **1**, **3**, and **5**; variable-temperature ¹H NMR spectra of compound **4**. This material is available free of charge via the Internet at <http://pubs.acs.org>.

OM0611608

(26) (a) te Velde, G.; Bickelhaupt, F. M.; Baerends, E. J.; Fonseca Guerra, C.; Van Gisbergen, S. J. A.; Snijders, J. G.; Ziegler, T. *J. Comput. Chem.* **2001**, *22*, 931. (b) Fonseca Guerra, C.; Snijder, J. G.; te Velde, G.; Baerends, E. J. *Theor. Chim. Acc.* **1998**, *99*, 391. (c) *ADF2005.01*, SCM; Theoretical Chemistry, Vrije Universiteit: Amsterdam, The Netherlands, <http://www.scm.com>.

(27) (a) van Lenthe, E.; Baerends, E. J.; Snijders, J. G. *J. Chem. Phys.* **1993**, *99*, 4597. (b) van Lenthe, E.; Baerends, E. J.; Snijders, J. G. *J. Chem. Phys.* **1994**, *101*, 9783. (c) van Lenthe, E.; Baerends, E. J.; Snijders, J. G. *J. Chem. Phys.* **1996**, *105*, 6505. (d) van Lenthe, E.; van Leeuwen, R.; Baerends, E. J.; Snijders, J. G. *Int. J. Quantum Chem.* **1996**, *57*, 281. (e) van Lenthe, E.; Ehlers, A.; Baerends, E. J. *J. Chem. Phys.* **1999**, *110*, 8943.

(28) Vosko, S. H.; Wilk, L.; Nusair, M. *Can. J. Phys.* **1980**, *58*, 1200.

(29) Becke, A. D. *Phys. Rev. A* **1988**, *38*, 3098.

(30) Perdew, J. P. *Phys. Rev. B* **1986**, *33*, 8822.